Thermopower in transition-metal perovskites

Wataru Kobayashi ●[*]

Division of Physics, Faculty of Pure and Applied Sciences, University of Tsukuba, Ibaraki 305-8571, Japan
and Tsukuba Research Center for Energy Materials Science (TREMS), University of Tsukuba, Ibaraki 305-8571, Japan

High-temperature thermopower is interpreted as entropy that a carrier carries. Owing to spin and orbital degrees of freedom, a transition-metal perovskite exhibits large thermopower at high temperatures. In this paper, we revisit the high-temperature thermopower in the perovskites to shed light on the degrees of freedom. Thus, we theoretically derive an expression of thermopower in one-dimensional octahedral-MX_6-cluster chain using linear-response theory and electronic structure calculation of the chain based on the tight-binding approximation. The derived expression of the thermopower is consistent with the extended Heikes formula and well reproduces experimental data of several perovskite oxides at high temperatures. In this expression, a degeneracy of many-electron states in an octahedral ligand field (which is characterized by the multiplet term) appears instead of the spin and orbital degeneracies. Complementarity in between our expression and the extended Heikes formula is discussed.

DOI: [10.1103/PhysRevB.104.245108](https://doi.org/10.1103/PhysRevB.104.245108)

I. INTRODUCTION

Transition-metal (M) oxides are one of fascinating quantum many-body systems, which exhibit a Mott insulating state [1], a spin-state crossover [2], peculiar magnetism accompanied by orbital ordering [3], high-temperature superconductivity [4], huge magnetoresistance [5], large thermopower [6], exotic superconductivity [7–9], multiferroicity [10], a spin-orbit related Mott insulating state [11], spin frustration (possibly spin liquid) [12], and other relativistic effects, such as Weyl semi metallic state [13]. A model material of the transition-metal oxides is a $3d$-transition-metal perovskite oxide expressed as $Ln_{1-x}Ae_xMO_3$ $[0 \leqslant x \leqslant 1]$, where Ln, Ae, and O represent lanthanide, alkali-earth-metal, and oxygen, respectively. This system has been extensively studied. In particular, metal-insulator transition (MIT) was deeply understood in terms of filling, bandwidth, and dimensional controls [14]. The filling control is given by a substitution of the Ae^{2+} ion for the Ln^{3+} ion (hole doping). The bandwidth (W) is controlled by the ionic radius (r_A) of the element at the A site. Smaller r_A causes a smaller M-O-M bond angle, which realizes smaller W. Tolerance factor (τ) is a function of r_A and a measure of strain in the perovskite structures. For $\tau \sim$ 0.9–1.0, the cubic structure with the M-O-M bond angle of 180° realizes. With decreasing r_A as $La^{3+} \rightarrow Pr^{3+} \rightarrow \cdots \rightarrow Y^{3+} \rightarrow Lu^{3+}$ and $Ba^{2+} \rightarrow Sr^{2+} \rightarrow Ca^{2+}$, τ decreases which causes a decrease in W. A ratio ($\frac{U}{W}$) of on-site Coulomb interaction (U) to W is a key parameter, which gives a quantum critical point of the metal-insulator transition. Revealing electronic structures in the $3d$-transition-metal perovskite oxides is generally difficult because of the electron correlation. The Hubbard model [15] is a well-known model that duplicates the MIT in the strongly correlated systems [14,16].

Thermopower (S) is a phenomenological transport coefficient and is defined as a temperature (T) derivative of thermoelectric voltage (V) as $S \equiv -\frac{dV}{dT}$ and can be applied for thermoelectric energy conversion [17]. Thermopower at the high-temperature limit in the quantum many-body systems is interpreted as entropy that a carrier carries in a regime of linear-response theory with the Hubbard model [18,19]. Chaikin and Beni generalized Heikes formula [19] to explain thermopower of interacting Fermi systems with spin and explained thermopower of a strongly correlated p-electron system (one-dimensional organic conductor) with spin entropy term $-\frac{k_B}{e} \ln 2$ [19]. Furthermore, Doumerc extended the formula to apply for a system containing a mixed valent cation $M^{n+}/M^{(n+1)+}$ using spin multiplicity $(2S_n + 1)$ [20]. Marsh and Parris again extended the formula to take into account the orbital degeneracy and qualitatively explained thermopower of $LaCrO_3$ [21], $LaMnO_3$ [22], and their related perovskite systems. Koshibae *et al.* also explained the large thermopower of $NaCo_2O_4$ using the spin and orbital degrees of freedom and proposed application of their theory to Co perovskite oxides [23]. In their theories, such degrees of freedom are introduced by counting a number of cases in the many-electron configuration in e_g and t_{2g} orbitals, and they seem to work well. To further consider the degrees of freedom, we derive a similar formula constructed from many-electron states in the MX_6 cluster with an octahedral ligand field where X represents ligand element without the use of a one-band Hubbard model (see Fig. 1).

In this paper, we construct thermopower of one-dimensional MX_6-cluster-chain model targeting the $3d$-transition-metal perovskite oxides with $\frac{U}{W} \gg 1$. In a derived expression of the thermopower, we find that a degener-
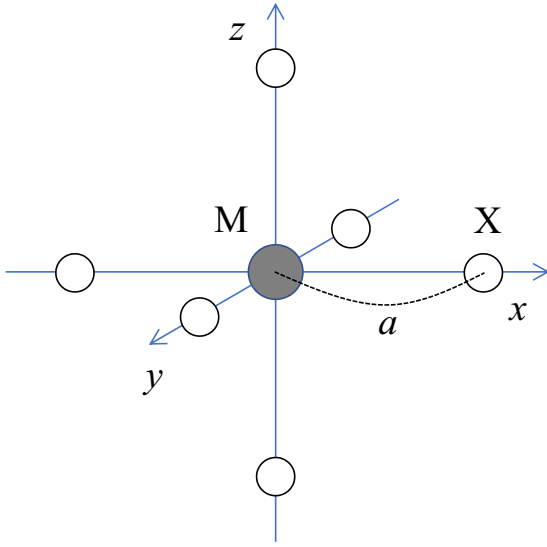
─────────
*kobayashi.wataru.gf@u.tsukuba.ac.jp

FIG. 1. Schematic of the MX_6 octahedron with O_h symmetry. The white circle represents a ligand (X) with its charge of $-Ze$, where Z and e represent positive integer and charge unit, respectively. d electrons in $3d$-transition-metal element (M) feel the octahedral ligand field.

acy of many-electron states in the MX_6-cluster is included instead of the degeneracies of the spin and the orbital. We will discuss the relation between spin and orbital degrees of freedom and the degeneracy of the many-electron states. We further apply our formula to experimental data of several $3d$-transition-metal perovskite oxides. Lastly, effects of spin-orbit interaction and Jahn-Teller distortion on the thermopower and further possible application of our theory will be discussed in Sec. III G.

II. METHODS

In this section, first, we briefly review the crystal- (ligand-) field theory. We see many d-electron states in the octahedral ligand field, term symbol, and how to count a degeneracy of the states that is represented by the term symbol. Second, we explain the tight-binding approximation (molecular-orbital theory) for the construction of the electronic structure of the periodically aligned one-dimensional MX_6-cluster-chain system (hereafter, the cluster-chain model. See Fig. 2). Third, we derive an expression of thermopower at the high-temperature limit for the cluster-chain model in a regime of linear-response theory. Last, we discuss complementarity in between the extended Heikes formula and our expression.
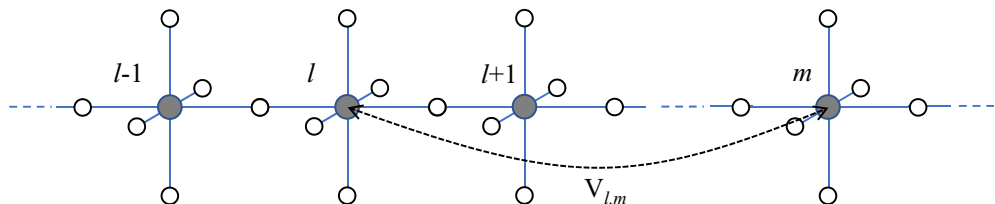
A. Crystal-field theory

To calculate physical properties of solids, we generally need to treat its electronic structure correctly taking into account periodicity of the crystal. However, if on-site Coulomb interaction (U) is much larger than interatomic transfer integral (t), we may discuss the physical properties of the crystal based on the atomic electronic states. Effects from other atoms can be treated as a crystal field or a ligand field which includes hybridization with p orbitals of the ligands.

Here, we briefly review the crystal-field theory (CFT). CFT describes a breaking of a degeneracy of electron orbital states (d or f orbital states) of an atom (or ion) due to a static electric field produced by a surrounding charge distribution. Suppose d electrons of the atom (or the ion) are surrounded by six negative charges ($-Ze$, Z as a positive integer and e as a charge unit) at $\boldsymbol{R}_k = (a, 0, 0)$, $(0, a, 0)$, $(0, 0, a)$, $(-a, 0, 0)$, $(0, -a, 0)$, and $(0, 0, -a)$. Then, the Hamiltonian (H_n) of the n d electrons, where n is a number of d electrons is described as

$$H_n = \left(\sum_{i=1}^{n} \frac{\boldsymbol{p}_i^2}{2m_e} + v_{\text{core}}(r_i) + v_{\text{CF}}(r_i) \right) + \sum_{j>i=1}^{n} \frac{e^2}{r_{i,j}}, \quad (1)$$

where m_e, $\boldsymbol{p}_i$, $r_i = |\boldsymbol{r}_i|$, and $r_{i,j} = |\boldsymbol{r}_i - \boldsymbol{r}_j|$ represent electron mass, momentum of the ith electron, distance in between a position of the ith electron and the origin, and relative distance in between $\boldsymbol{r}_i$ and $\boldsymbol{r}_j$. $v_{\text{core}}(r_i)$ is a potential of atom and valence electrons (central force field approximation), $v_{\text{CF}}(r_i)$ is a crystal-field $v_{\text{CF}}(r_i) = \sum_{k=1}^{6} \frac{Ze^2}{|\boldsymbol{R}_k - r_i|}$, and the last term represents electron interaction between d electrons. When $n = 1$, the fourth term vanishes which results in well-known $d_{x^2-y^2}$ (we denote this as ϕ_v or v), $d_{3z^2-r^2}$ (ϕ_u or u), d_{xy} (ϕ_ζ or ζ), d_{yz} (ϕ_ξ or ξ), and d_{zx} (ϕ_η or η) wave functions are obtained. Note that these wave functions are real functions. For $v_{\text{core}}(r_i) = -\frac{e^2}{r_i}$, the energy gap in between e_g and t_{2g} orbitals is evaluated as $10Dq$, where $D = \frac{35Ze}{4a^5}$ and $q = \frac{2e}{105} \langle r^4 \rangle$ (the average of r^4, $\langle r^4 \rangle \equiv \int |R_{nd}|^2 r^4 r^2 dr$, R_{nd} is the radial wave function of nd states.) [24]. Parameters Z and a can tune the energy gap. In this sense, Z and a can express the material's characteristics. Thus, under octahedral coordination, fivefold d orbitals split into threefold t_{2g} and twofold e_g orbitals.

When $n > 1$, electron correlation should be taken into account. Tanabe and Sugano have constructed solutions for n d electrons ($1 \leq n \leq 9$) in the crystal field (strong crystal-field limit) [25,26]. As a result, the many-electron state is found to be expressed as a linear combination of Slater determinants including ϕ_u(or u), $\phi_v(v)$, $\phi_\zeta(\zeta)$, $\phi_\xi(\xi)$, $\phi_\eta(\eta)$ (spin up), $\bar{\phi}_u$(or $\bar{u}$), $\bar{\phi}_v(\bar{v})$, $\bar{\phi}_\zeta(\bar{\zeta})$, $\bar{\phi}_\xi(\bar{\xi})$, $\bar{\phi}_\eta(\bar{\eta})$ (spin down).

FIG. 2. Schematic of the periodically aligned one-dimensional N-cluster chain. The broken arrow represents intercluster interaction in between lth and mth clusters ($V_{l,m}$).

TABLE I. Number of d electrons (d_n), electronic configuration, spin state, ground multiplet term ($^{2S+1}\Gamma$), and degeneracy of $^{2S+1}\Gamma$ (Γ). The ground terms were referred from Ref. [26]. * :These intermediate states are excited states in the Tanabe-Sugano diagram.

d^n	Electronic configuration	Spin state	Ground multiplet term ($^{2S+1}\Gamma$)	Degeneracy of $^{2S+1}\Gamma$ (Γ)
d^0	$(t_{2g})^0(e_g)^0$	–	$^1A_{1g}$	1
d^1	$(t_{2g})^1(e_g)^0$	–	$^2T_{2g}$	6
d^2	$(t_{2g})^2(e_g)^0$	–	$^3T_{1g}$	9
d^3	$(t_{2g})^3(e_g)^0$	–	$^4A_{2g}$	4
d^4	$(t_{2g})^3(e_g)^1$	High spin	^5E_g	10
	$(t_{2g})^4(e_g)^0$	Low spin	$^3T_{1g}$	9
d^5	$(t_{2g})^3(e_g)^2$	High spin	$^6A_{1g}$	6
	$(t_{2g})^4(e_g)^1$	*Intermediate spin	$^{*4}T_{1g}$	12
	$(t_{2g})^5(e_g)^0$	Low spin	$^2T_{2g}$	6
d^6	$(t_{2g})^4(e_g)^2$	high spin	$^5T_{2g}$	15
	$(t_{2g})^5(e_g)^1$	*Intermediate spin	$^{*3}T_{1g}$	9
	$(t_{2g})^6(e_g)^0$	Low spin	$^1A_{1g}$	1
d^7	$(t_{2g})^5(e_g)^2$	High spin	$^4T_{1g}$	12
	$(t_{2g})^6(e_g)^1$	Low spin	^2E_g	4
d^8	$(t_{2g})^6(e_g)^2$	–	$^3A_{2g}$	3
d^9	$(t_{2g})^6(e_g)^3$	–	^2E_g	4
d^{10}	$(t_{2g})^6(e_g)^4$	–	$^1A_{1g}$	1

Write the many-electron state as $\Phi_n(t_2^p e^q{:}^{2S+1}\Gamma M_s \gamma)$, where p and q ($n = p + q$) represent a number of electrons at t_2 orbitals (ζ, η, ξ) and e orbitals (u, v), $^{2S+1}\Gamma$ represents a multiplet term, M_s is an eigenvalue of total spin angular momentum (S_z), and γ represents the ground function of irreducible representation Γ (e.g., $\Gamma = T_2$, $\gamma = \xi, \eta, \zeta$). As an example, we briefly treat $n = 2$. A number of cases for the $(t_2)^2$ configuration is 15 ($=_6C_2$). Thus, we can provide 15 Slater determinants as $|\xi\eta|, |\bar{\xi}\bar{\eta}|, \ldots,$ and $|\xi\bar{\xi}|$. Then, using a linear combination (Φ_2) of these 15 Slater determinants, $\langle\Phi_2|\frac{e^2}{r_{i,j}}|\Phi_2\rangle$ can be diagonalized, then we obtain $\Phi_2 = \Phi_2(t_2^2{:}^{2S+1}\Gamma M_s \gamma)$. This solution is further characterized by a multiplet term which represents symmetry of the many-electron states under an octahedral ligand field. For example, $\Phi_2(t_2^2{:}^3T_1 M_s = 1\gamma) = |\xi\eta|, |\eta\zeta|,$ and $|\zeta\xi|$. $\Phi_2(t_2^2{:}^3T_1 M_s = 0\gamma) = \frac{1}{\sqrt{2}}\{|\xi\bar{\eta}|-|\eta\bar{\xi}|\}, \frac{1}{\sqrt{2}}\{|\eta\bar{\zeta}|-|\zeta\bar{\eta}|\},$ and $\frac{1}{\sqrt{2}}\{|\zeta\bar{\xi}|-|\xi\bar{\zeta}|\}$. $\Phi_2(t_2^2{:}^3T_1 M_s = -1\gamma) = |\bar{\xi}\bar{\eta}|, |\bar{\eta}\bar{\zeta}|,$ and $|\bar{\zeta}\bar{\xi}|$. These nine functions are energetically degenerate. A degeneracy of the multiplet term $^{2S+1}\Gamma$ is a product of spin multiplicity ($2S + 1$) and Γ_0. Γ_0 is a dimensional number of irreducible representation [1 for $A(B)$, 2 for E, and 3 for T]. Thus, a degeneracy of $^3T_1$ is expressed as $3 \times 3 = 9$.

Next, let us see briefly the multiplet theory of an atom [27]. The many-electron state of a free ion is expressed using term symbol ^{2S+1}L, where L is total orbital angular momentum ($L = S, P, D, F, G, \ldots$ corresponds to 0, 1, 2, 3, 4, …, respectively.). A degeneracy of the many-electron state is expressed as $(2S + 1)(2L + 1)$. For example, d^5 has 252-fold degeneracies ($=_{10}C_5$), however, under the spherical Coulomb potential, it splits, and the ground term becomes ^6S. Thus, the degeneracy decreases from 252 to 6. Under a weak-crystal field, these ground states remain alive and expressed as $^6A_{1g}$. As shown above, for the strong crystal-field limit, we see how to construct many-electron states by Tanabe and Sugano. By connecting the weak-crystal-field limit [27], Tanabe

and Sugano constructed the Tanabe-Sugano diagram [25,26]. Each state in the diagrams is labeled by term symbols, which shows symmetry of the many-electron states under a ligand field and its degeneracy of each state. Thus, the Tanabe-Sugano diagram gives information on the degeneracies of d-electron wave functions in the octahedral ligand field. The number of the degeneracy can be read from the term symbol. Table I lists the ground multiplet term and degeneracy (Γ) that the multiplet term represents for $0 \leqq n \leqq 10$. Note that the intermediate spin states are excited states in the Tanabe-Sugano diagram. In our theory, the degeneracy of the ground multiplet term plays an important role. Ligand field theory succeeded in explaining several physical properties, such as thermochemical properties (hydration enthalpies) and geometric distortions (Jahn-Teller distortion and spinel structures), various spectroscopies of transition-metal coordination complexes, in particular, optical spectra (colors), magnetic properties (spin-orbit-coupling related magnetism), and so on [24,27].

B. Electronic structure of the one-dimensional N-cluster-chain model

As a next step, let us construct the one-dimensional N-cluster-chain model (N is a number of clusters).

We assume a tight-binding approximation of the clusters. The Hamiltonian of the cluster-chain model is described as

$$H_N = \sum_{l=1}^{N} H_{n_l l} + \sum_{l \neq m} V_{l,m}, \qquad (2)$$

where $H_{n_l l}$ represents the Hamiltonian of the lth cluster [equivalent to Eq. (1)], n_l represents a number of d electrons at the lth cluster, and intercluster interaction in between lth and mth clusters is introduced as $V_{l,m}$ (see Fig. 2). The many-electron wave function of the N-cluster chain is constructed by a linear combination of one of the degenerated wave functions

of the lth cluster $[\Phi_{nl}(t_2^p e^q:{}^{2S+1}\Gamma M_s\gamma)]$ as

$$\Psi_N = \sum_{l=1}^{N} c_l \Phi_{nl}\left(t_2^p e^q:{}^{2S+1}\Gamma M_s\gamma\right), \qquad (3)$$

where c_l is a normalized constant. Since both H_N and Ψ_N are real functions, the matrix elements are expressed as real symmetric matrices,

$$\langle \Psi_N|H_N|\Psi_N\rangle$$

$$= \begin{pmatrix} \vdots \\ \vdots \\ c_l \\ \vdots \\ \vdots \\ c_m \\ \vdots \end{pmatrix}^t \begin{pmatrix} \ddots & & & & & & \\ & E_{l-1} & & & & & \\ \cdots & t_{l-1,l} & E_l & t_{l,l+1} & \cdots & t_{l,m} & \cdots \\ & & \vdots & E_{l+1} & & & \\ & & \vdots & & \ddots & & \\ & & t_{m,l} & & & \ddots & \\ & & \vdots & & & & \ddots \end{pmatrix}$$

$$\times \begin{pmatrix} \vdots \\ \vdots \\ c_l \\ \vdots \\ \vdots \\ c_m \\ \vdots \end{pmatrix}, \qquad (4)$$

where E_l is one cluster energy $\langle \Phi_{nl}(t_2^p e^q:{}^{2S+1}\Gamma M_s\gamma|H_{nl}|\Phi_{nl}(t_2^p e^q:{}^{2S+1}\Gamma M_s\gamma\rangle$ and $t_{l,m}$ is the intercluster interaction energy $\langle \Phi_{nl}(t_2^p e^q:{}^{2S+1}\Gamma M_s\gamma|V_{l,m}|\Phi_{nmm}(t_2^p e^q:{}^{2S+1}\Gamma M_s\gamma\rangle$. $t_{l,m} = t_{m,l}$ is trivial as $V_{l,m}$ is a two-body Coulomb interaction. Thus, using a proper orthogonal matrix, this matrix can be exactly diagonalized, then eigenvalues and eigenstates of the N-cluster chain are exactly determined.

Now, let us apply this general discussion to the M^{3+}/M^{4+} mixed-valent system. We set $E_l = E_3$ or E_4 where it is the energy of a cluster with M^{3+} or M^{4+}. A number of M^{4+} clusters is M, and a number of M^{3+} clusters is $N - M$. Under this condition, we take into account the nearest-neighbor intercluster interaction, namely, $t_{l-1,l} \neq 0$, $t_{l,l+1} \neq 0$, and $t_{l,m} = 0$ ($m \neq l-1$ or $l+1$). Total energy $E(d^n)$ of the MX_6 cluster with d^n is $E(d^n) = E_0 + n\epsilon_d^0 + \frac{n(n-1)}{2}\bar{U}$, where E_0 is the total energy of the d^0 cluster, ϵ_d^0 is one-electron energy, and $\bar{U}$ is the average of Coulomb and exchange energies in between two electrons. Thus, $E(d^n) - E(d^{n-1})$ becomes $\epsilon_d^0 + \bar{U}(n-1)$. Then, the E_3-E_4 value can be regarded as a Hubbard U. Thus, this approximation is regarded as the Hubbard-like model. Then, the narrow bandlike feature with the width of $W \sim t_{l-1,l}, t_{l,l+1}$ will be formed around E_3 and E_4. Using a small intercluster interaction, thus, $\frac{U}{W} \gg 1$ can be realized.

Here, we briefly discuss $t_{l-1,l}$ and $t_{l,l+1}$ from the microscopic orbital point of view. The values of the hopping integrals in between s, p, and d orbitals for the (l', m', n') direction were already calculated as the Slater-Koster parameter in Table I of Ref. [28]. According to Slater and Koster, the hopping integral in the high-symmetric one-dimensional model [two centers are connected along the directions of

(1, 0, 0), (0, 1, 0), (0, 0, 1)] automatically becomes zero for several orbital cases. Thus, to avoid the zero hopping integral, the tilted zigzag chain structure as seen in the $GdFeO_3$-type structure is effective. Then, all the hopping in between d orbitals become possible, which means that electron can move from one edge to another edge through the crystal with energy, although the value of the hopping integral depends on the orbital. Then, if one uses a condition of $W \ll k_B T \ll U$ (highly flat-band situation) where k_B and T represent the Boltzmann constant and temperature, all the hopping can almost equally occur with use of the help of the thermal energy much larger than the bandwidth. Thus, local degeneracy in the MX_6 octahedron can be kept even if such a flat-band structure is constructed by the cluster chain. Since the orthorhombic $GaFeO_3$-type perovskite has three inequivalent directions (a, b, and c), explicitly speaking, hopping integral along the one axis is slightly different from the ones along the other axes. However, the condition of $W \ll k_B T \ll U$ can make the same local degeneracy along these axes. There are other structures composed by MX_6 octahedra. For example, edge-shared MX_6 octahedra can make a MX_2 layer with a triangular lattice. For this case, t_{2g}-t_{2g} hopping would be preferable compared with e_g-e_g hopping. However, if such a material satisfies the condition of $W \ll k_B T \ll U$, we can also use the local degeneracy to apply our theory to such a material.

C. Thermopower of the one-dimensional N-cluster-chain model

Since the electronic structure of the N-cluster chain is exactly determined, now we can define energy flux (J_q) and current flux (J). Then, we can discuss thermopower. The expression of the thermopower is expressed as

$$S = -\frac{k_B}{e}\left[\frac{1}{k_B T}\left(\frac{J_q}{J}\right)_{\nabla T=0} - \frac{\mu}{k_B T}\right], \qquad (5)$$

where μ represents the chemical potential [22]. When a material can be well described as a band picture (mean-field approximation), the Boltzmann equation regime works well. Based on the band calculation and the Boltzmann equation, Singh reproduced a large thermopower ($\sim$110 μV/K) of $NaCo_2O_4$ at 300 K [29]. Even if the band picture does not work well (example correlated hopping conduction), by carefully taking into account interactions in a Hamiltonian, Kubo-Luttinger formalism [30,31] works well. Recently, Matsuura *et al.* explained large thermopower of ($\sim$20 mV/K) at around 10 K taking into account electron-phonon interaction [32]. Thermopower of the strongly correlated electron system including 3d-transition-metal perovskite oxide has been qualitatively explained based on the single-band Hubbard model [21–23]. And introduced degeneracies of spin and orbital play an important role. To further consider the degrees of freedom, we evaluate the thermopower of the one-dimensional N-cluster chain.

First, we consider the term $\frac{1}{k_B T}\left(\frac{J_q}{J}\right)$. $\left(\frac{J_q}{J}\right)$ is an averaged energy that a carrier carries. For our model, against an external field [such as electric-field E or temperature gradient (∇T)] as perturbation, most of the initial states excite within the bandwidth W. So that we may evaluate $\frac{1}{k_B T}\left(\frac{J_q}{J}\right)$ as $\sim \frac{W}{k_B T}$. Thus,

for $W \ll k_B T \ll U$ at the limit of $T \to \infty$,

$$\lim_{T \to \infty} S = \frac{\mu}{eT} = -\frac{1}{e}\left(\frac{\partial s}{\partial N_e}\right)_{E,V}, \quad (6)$$

where s, N_e, E, and V represents entropy, electron number, total energy, and volume in the N-cluster chain, respectively. We call this the high-temperature limit value. According to the t-J model by Koshibae and Maekawa [33], the high-temperature limit value is almost realized at around $\frac{k_B T}{t} \sim 5$. According to one-dimensional Hubbard model analysis, S almost saturates at around $\frac{k_B T}{t} \sim 1$ [34]. This is also consistent with the assumption of our method [$(\frac{J_q}{J}) \sim W$].

When $V_{l-1,l}$ and $V_{l,l+1} \sim W$, although all the eigenstates and eigenvalues of the N-cluster-chain system are exactly determined, calculation of the entropy (counting of a number of degenerated eigenstates at total energy E) is highly complicated. Thus, we further consider the limit of $W \to 0$ (namely, $V_{l,m} \to 0$). Here, we would like to note the difference in between the zero-$\frac{W}{k_B T}$ limit and the zero-W limit. The zero-$\frac{W}{k_B T}$ limit does not mean $W = 0$. To evaluate an exact number of degenerated eigenstates at E, we further impose strong limitation on our theory.

At the $W = 0$ limit, the N-cluster-chain system becomes simple, namely, a periodically aligned one-dimensional noninteracting cluster. Then, the wave function of the system is described as a direct product of the wave function of the lth cluster [$\Phi_{n_l l}(t_2^p e^q{:}^{2S+1}\Gamma M_s \gamma)$],

$$\Psi_N = \prod_{l=1}^{N} \Phi_{n_l l}\left(t_2^p e^q{:}^{2S+1}\Gamma M_s \gamma\right). \quad (7)$$

Total energy E of the system is expressed as $E = (N - M)E_3 + ME_4$. A number of electrons N_e is expressed as $N_e = (N - M)n_3 + Mn_4$, where n_3 (n_4) represents a number of electrons in a cluster with M^{3+} (M^{4+}). Since $n_3 - n_4 = 1$, N_e becomes $N_e = Nn_3 - M$. Then, a number (g) of degenerated eigenstates at E is evaluated as

$$g = \Gamma_3^{N-M}\Gamma_4^{M}\frac{N!}{M!(N-M)!}, \quad (8)$$

where Γ_3 (Γ_4) represents degeneracy of many-electron states in a M^{3+} (M^{4+}) cluster at E_3 (E_4). Using Boltzmann principle of entropy $s = k_B \ln g$, thermopower at the high-temperature limit becomes

$$S = -\frac{k_B}{e}\left(\frac{\partial \ln g}{\partial N_e}\right)_{E,V} = \frac{k_B}{e}\left(\frac{\partial \ln g}{\partial M}\right)_{E,V}. \quad (9)$$

By substituting Eq. (8) into Eq. (9) and using Stirling's approximation,

$$S = -\frac{k_B}{e}\ln\left(\frac{\Gamma_3}{\Gamma_4}\frac{x}{1-x}\right), \quad (10)$$

is obtained as a final formula where x is defined as $\frac{M}{N}$.

D. Comparison with the extended Heikes formula

The extended Heikes formula expresses thermopower in the d-electron system [20–23]. The total number of config-

urations for $t \ll k_B T \ll U$ will be written as

$$g = g_3^{N_A - M}g_4^{M}\frac{N_A!}{M!(N_A - M)!}, \quad (11)$$

where N_A is a system size, M is the number of M^{4+} ions. g_3 and g_4 are defined as the number of electronic configurations of M^{3+} and M^{4+} ions (spin and orbital degrees of freedom). Substituting Eq. (11) for Eq. (9), then, the thermopower is obtained as

$$S = -\frac{k_B}{e}\ln\left(\frac{g_3}{g_4}\frac{x}{1-x}\right), \quad (12)$$

where x is a ratio of the M^{4+} ion to the system size N_A ($x = \frac{M}{N_A}$) [21–23]. Equations (11) and (12) are almost identical to Eqs. (8) and (10).

Now let us compare g_i with Γ_i ($i = 3, 4$). According to Marsh and Parris [21,22], and Koshibae *et al.* [23], a number of n d-electron configurations in e_g and t_{2g} orbitals with the use of spin multiplicity ($2S + 1$), and orbital degeneracy is calculated using a number of cases. When t_{2g} or e_g orbitals ares partially occupied, the direct product of the totally symmetric representation and irreducible representation becomes $^1A_{1g} \times {}^{2S+1}\Gamma = {}^{2S+1}\Gamma$. So that degeneracy of the orbital can be a dimension of Γ ($\Gamma = A$ or $B \to 1$, $E \to 2$, $T \to 3$). Thus, degeneracy of the ground multiplet term becomes equal to degeneracies of spin and orbital. However, if both e_g and t_{2g} orbitals are partially occupied (e.g., the excited state, such as the intermediate spin state of Co^{3+}), the product of representations becomes $E_g \times T_{2g} = T_{1g} + T_{2g}$ in O_h symmetry. Then, the number of the configurations differs from the degeneracies of spin and orbital (e.g., $t_{2g}^4 e_g^1$ ($S = \frac{3}{2}$) $\to$ spin multiplicity is 4, orbital degeneracy is 3 for t_{2g}, 2 for e_g, thus, degeneracies of spin and orbital become 24 [23]) because Coulomb interaction split 24 states into $12 + 12$ states depending on the symmetry of the many electron states. However, if these states are regarded as degenerated due to some ignored interaction in the crystal-field approximation [23], g_i becomes identical to Γ_i for $0 \leqslant n \leqslant 10$.

Next, we see a difference in the derivations. Marsh and Parris calculated the chemical potential with the use of the "grand canonical ensemble" [21,22]. Koshibae *et al.,* calculated the chemical potential with the use of the "microcanonical ensemble" [23]. Since different ensembles lead to the same expression, the extended Heikes formula is validly constructed based on thermodynamics and quantum statistical mechanics. Our formula is consistent with their results as shown above. We derived our expression of S by considering the microcanonical ensemble of exact many-electron states at total energy E. Since the extended Heikes formula and our formula are almost identical, these formulas are complementary.

Thanks to the comparison shown above, now we recognize an important feature. When thermopower of the metallic perovskite with magnetic interaction is discussed, the Heikes formula has an advantage to guess the degeneracy of the many-electron states. Since it is highly difficult to exactly know the eigenstates and the eigenvalues of correlated metallic states ($U \ll k_B T$), our method is not applicable. Thus, thermopower in the correlated metallic state even seems to

be reproduced by the spin and orbital degeneracies. S at the high-temperature limit is entropy that a carrier carries. So that the experimental data at high temperatures generally gives important information about the entangled entropy. The extended Heikes formula is also applicable for the even frustrated state with the triangular lattice.

III. COMPARISON WITH EXPERIMENTS AND DISCUSSION

As shown in the Introduction, a condition $W \ll k_B T \ll U$ is realized in a $3d$-transiton-metal perovskite with low τ (small W) [14]. At $V_{l,m} \sim 0$; $(W \ll k_B T)$, many of the systems exhibit a paramagnetic insulating state. Thus, the $3d$-transition-metal perovskite with insulating (semiconducting) conductivity due to hopping conduction and paramagnetism will exhibit almost saturated thermopower at high temperatures. We investigate the x dependence of thermopower at high temperatures from previous works in which the material satisfies this condition. Now, let us compare experimental data with our expression. (Note that the proper data are not found after d^7 in the literature.)

A. The d^0/d^1 system

The d^0/d^1 system corresponds to the Ti^{4+}/Ti^{3+} system. SrTiO$_3$ is a band insulator, and with La doping (electron doping), Sr$_{1-x}$La$_x$TiO$_3$ $(0.0 \leqslant x \leqslant 0.1)$ exhibits paramagnetic metallic states. Thermopower of the system exhibits a negatively large value, which is highly expected as a n-type thermoelectric material [35]. With $La^{3+} \rightarrow Pr^{3+}$, Pr$_{1-x}Sr_xTiO_3$ exhibits an insulating state possibly due to narrower W than that of La$_{1-x}$Sr$_x$TiO$_3$.

Figure 3(a) shows the x dependence of thermopower in Pr$_{1-x}$Sr$_x$TiO$_3$ $(0.7 \leqslant x \leqslant 0.98)$ at 1200 K [36]. With $\Gamma_3 = 6$ and $\Gamma_4 = 1$, Eq. (10) is drawn as a broken line. The x dependence of the thermopower is referred from Fig. 5 in Ref. [36]. They still gradually increase even at 1200 K due to rather large W of this system. However, the thermopower data seem to saturate at higher temperatures. So that we plot these data in Fig. 3(a) with the theoretical curve.

B. The d^1/d^2 system

The filling-controlled Mott transition system La$_{1-x}$Sr$_x$VO$_3$[37] is a typical d^1/d^2 system $(V^{4+}/V^{3+}$ system). According to the schematic metal-insulator diagram in Fig. 65 of Ref. [14], this system has a rather large W. So that thermopower of this system does not indicate its saturation (they exhibit strong T dependence) even at high temperatures (1250 K). Thus, our expression cannot treat this result. Combining the extended Heikes formula and dynamical mean-field theory calculation on the single-band Hubbard model, Uchida *et al.*, [37] indicate that the thermopower merges a value expected by the Heikes formula for the $U \ll k_B T$ limit at high temperatures.

C. The d^2/d^3 system

La$_{1-x}$Sr$_x$CrO$_3$ is a typical d^2/d^3 system $(Cr^{4+}/Cr^{3+}$ system) which exhibits insulating T dependence, and its ther-
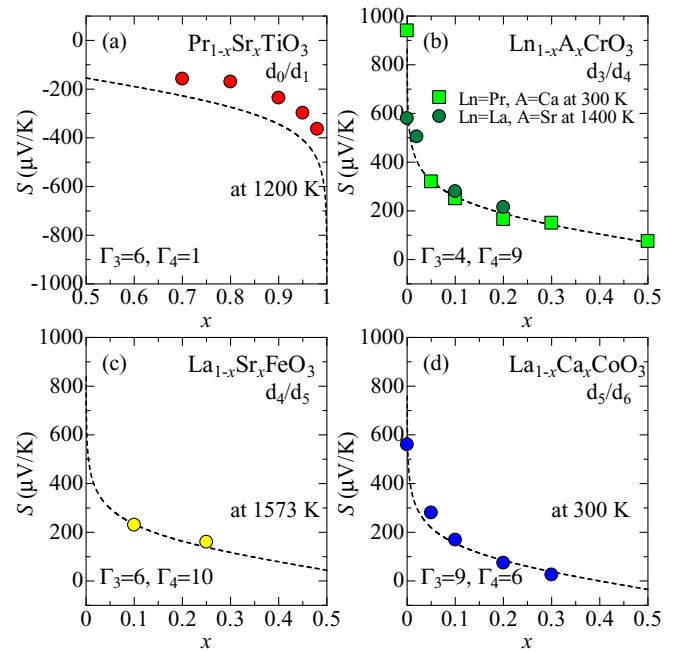

FIG. 3. x dependence of thermopower in (a) the d_0/d_1 system Pr$_{1-x}$Sr$_x$TiO$_3$ at 1200 K [36], (b) the d_3/d_4 systems La$_{1-x}$Sr$_x$CrO$_3$ at 1400 K [38], and Pr$_{1-x}$Ca$_x$CrO$_3$ at 300 K [39], (c) the d_4/d_5 system La$_{1-x}$Sr$_x$FeO$_3$ at 1573 K [42], and (d) the d_5/d_6 system La$_{1-x}$Ca$_x$CoO$_3$ at 300 K [44]. In each figure of (a)–(d), Eq. (10) is drawn as a broken line. Numbers of Γ_3 and Γ_4 are displayed in each figure.

mopower almost saturates above 1000 K [38]. Pr$_{1-x}$Ca$_x$CrO$_3$ [39] has a narrower W than that of La$_{1-x}$Sr$_x$CrO$_3$. The thermopower of this system almost saturates above 250 K. And the paramagnetic insulating state is realized above 250 K. Pal *et al.* [39] have shown that the x dependence of the thermopower is qualitatively explained by the extended Heikes formula. Marsh and Parris reproduced the thermopower of the La$_{1-x}$Sr$_x$CrO$_3$ [21] system at 1400 K by using their theory with degeneracies of spin and orbital $\beta_0 = 9$ and $\beta_1 = 4$. In Fig. 3(b), we replotted the data of La$_{1-x}$Sr$_x$CrO$_3$ [38] and Pr$_{1-x}$Ca$_x$CrO$_3$ [39] with Eq. (10).

D. The d^3/d^4 system

La$_{1-x}$Sr$_x$MnO$_3$ [22] and La$_{1-x}$Ca$_x$MnO$_3$ [22] are the typical model materials of the d^3/d^4 system $(Mn^{4+}/Mn^{3+}$ system). From extensive research of these systems, a rich phase diagram is obtained. Charge ordering, ferromagnetism due to strong magnetic coupling, Jahn-Teller instability, and phase separation cause the rich phases. Marsh and Parris explained the x dependence of the thermopower of these systems using their theory [22]. It seems to us that, in particular, $\Gamma_0 = 1$ (Γ_0: spin degeneracy) due to long-range magnetic coupling and $\Delta_{JT} \ll k_B T$, $U \ll k_B T$ cause weak x dependence of the thermopower below $x = 0.2$. Palstra *et al.*, also reported x dependence of the thermopower for La$_{1-x}$Ca$_x$MnO$_3$ and found almost x-independent values at 475 K [40]. Kobayashi *et al.*, reported x dependence of the thermopower of CaMn$_{3-x}$Cu$_x$Mn$_4$O$_{12}$ with a narrower M-O-M bond angle (=142°) and found almost x-independent

values at 1373 K [41]. They exhibit insulating T dependence of electrical conductivity possibly due to narrow-band width W. However, Jahn-Teller instability and short- and long-range magnetic interactions seem to cause the small almost x-independent thermopower.

E. The d^4/d^5 system

La$_{1-x}$Sr$_x$FeO$_3$ [42] is a typical d^4/d^5 system (Fe^{4+}/Fe^{3+} system). La$_{1-x}$Sr$_x$FeO$_3$ ($x = 0.1$ and 0.25) exhibit the paramagnetic insulating state [14]. The thermopower almost saturates for $x = 0.1$ above 1173 K. We plotted the data at 1573 K with $\Gamma_3 = 6$ and $\Gamma_4 = 10$ (for high spin) in Fig. 3(c).

F. The d^5/d^6 system

LaCoO$_3$ is well known as a spin-state crossover system [2]. With Sr doping, the system experiences MIT and shows a ferromagnetic metallic state. The Co-O-Co bond angle is smaller for $A =$ Ca than that for $A =$ Sr. La$_{1-x}$Sr$_x$CoO$_3$ [43,44] is a typical d^5/d^6 system (Co^{4+}/Co^{3+} system) and exhibits insulating temperature dependence of resistivity up to $x = 0.2$ although it is $x = 0.3$ for La$_{1-x}$Ca$_x$CoO$_3$. The thermopower seems to saturate around 300 K. (Note that at higher temperatures this system exhibits temperature-induced MIT. Toward the MIT, S decreases with T.) We replotted the thermopower data at 300 K in La$_{1-x}$Ca$_x$CoO$_3$ [44] with $\Gamma_3 = 9$ and $\Gamma_4 = 6$ (intermediate state for Co^{3+}, low spin state for Co^{4+}) in Fig. 3(d).

G. General discussion

As shown above, our formula well reproduces the thermopower of $3d$-transition-metal perovskite oxides with small W and large U without both short- and long-range magnetic couplings. Although the extended Heikes formula seems to be applicable even for the correlated metallic state with magnetic interaction at a limit of $U \ll k_B T$ (for V^{4+}/V^{3+} and Mn^{4+}/Mn^{3+} systems). In general, these conditions give weak x dependence of the thermopower and a rather small S value due to small spin degree of freedom (~ 1). Thus, entanglement in between other clusters works to decrease the thermopower. The Jahn-Teller effect and spin-orbit interaction can also be

treated within our regime beyond the present evaluation. For example, La$_{1-x}$Ca$_x$MnO$_3$ has Jahn-Teller instability. The distortion of the MnO$_6$ octahedron induces $^5E_g \rightarrow{}^5 A_{1g} +^5 B_{1g}$, namely, tenfold degeneracies becomes fivefold degeneracies with an energetically stable state and fivefold degeneracies with an unstable state. This effect is treated as $\Gamma_3 = 10 \rightarrow 5$ for the d^4/d^5 system. As shown here, these effects break the degeneracy of the many-electron states at any energy E, which gives smaller S values than that the present one. Presently, our theory is applied to only the compounds with MX_6 octahedra. However, for example, if one uses local degeneracy of another cluster, such as a tetrahedron, a triangular prism, and so on, one could discuss thermopower of the other structures with those clusters within the condition of $W \ll k_B T \ll U$, which is beyond the present paper. In addition, we would like to note that our theory can treat d^0 to d^{10} electrons, which includes other valences of the M ion.

IV. CONCLUSION

In conclusion, we widely investigate thermopower (at high temperatures) of $3d$-transition-metal perovskite oxides comparing the extended Heikes formula. We constructed an expression of the thermopower from many-electron electronic states of MX_6 (M: transition metal, X: ligand element) octahedral clusters and reproduced x dependence of the thermopower of several perovskites with $W \ll k_B T \ll U$ using a degeneracy of many-electron states that multiplet term represents at the total energy E. Comparison of our expression with the extended Heikes formula, complementarity of these formulas become clear. Thermopower in the correlated metallic state with small U and the magnetic coupling can be treated by the extended Heikes formula. This is highly efficient because without knowing the exact many-electron states, we can evaluate thermopower with considering the inner degrees of freedom. Even in transport, we see an importance of crystal symmetry, which regulates a value of thermopower.

[1] N. F. Mott, The basis of the electron theory of metals, with special reference to the transition metals, Proc. Phys. Soc., London, Sect. A **62**, 416 (1949).

[2] J. B. Goodenough, An interpretation of the magnetic properties of the perovskite-type mixed crystals La$_{1-x}$Sr$_x$CoO$_{3-\lambda}$, J. Phys. Chem. Solids **6**, 287 (1958).

[3] K. I. Kugel and D. I. Khomskii, The Jahn-Teller effect and magnetism: Transition metal compounds, Sov. Phys. Usp. **25**, 231 (1982).

[4] J. B. Bednorz and K. A. Muller, Possible high T_c superconductivity in the Ba-La-Cu-O system, Z. Phys. B: Condens. Matter **64**, 189 (1986).

[5] Y. Tokura, A. Urushibara, Y. Moritomo, T. Arima, A. Asamitsu, G. Kido and N. Furukawa, Giant magnetotransport phenomena in filling-controlled kondo lattice system: La$_{1-x}$Sr$_x$MnO$_3$, J. Phys. Soc. Jpn. **63**, 3931 (1994).

[6] I. Terasaki, Y. Sasago, and K. Uchinokura, Large thermoelectric power in NaCo$_2$O$_4$ single crystals, Phys. Rev. B **56**, R12685(R) (1997).

[7] Y. Maeno, H. Hashimoto, K. Yoshida, S. Nishizaki, T. Fujita, J. G. Bednorz, and F. Lichtenberg, Superconductivity in a layered perovskite without copper, Nature (London) **372**, 532 (1994).

[8] K. Takada, H. Sakurai, E. Takayama-Muromachi, F. Izumi, R. A. Dilanian, and T. Sasaki, Superconductivity in two-dimensional CoO$_2$ layers, Nature (London) **422**, 53 (2003).

[9] Y. Kamihara, T. Watanabe, M. Hirano, and H. Hosono, Iron-based layered superconductor La[O$_{1-x}$F$_x$]FeAs ($x = 0.05 - 0.12$) with $T_c = 26$ K, J. Am. Chem. Soc. **130**, 3296 (2008).

[10] T. Kimura, T. Goto, H. Shintani, K. Ishizaka, T. Arima, and Y. Tokura, Magnetic control of ferroelectric polarization, Nature (London) **426**, 55 (2003).

[11] B. J. Kim, H. Ohsumi, T. Komesu, S. Sakai, T. Morita, H. Takagi, and T. Arima, Phase-sensitive observation of a spin-orbital mott state in Sr_2IrO_4, Science **323**, 1329 (2009).

[12] K. Kitagawa, T. Takayama, Y. Matsumoto, A. Kato, R. Takano, Y. Kishimoto, S. Bette, R. Dinnebier, G. Jackeli, and H. Takagi, A spin-orbital-entangled quantum liquid on a honeycomb lattice, Nature (London) **554**, 341 (2018).

[13] T. Ohtsuki, Z. Tian, A. Endo, M. Halim, S. Katsumoto, Y. Kohama, K. Kindo, M. Lippmaa, and S. Nakatsuji, Strain-induced spontaneous Hall effect in an epitaxial thin film of a Luttinger semimetal, Proc. Natl. Acad. Sci. USA **116**, 8803 (2019).

[14] M. Imada, A. Fujimori, and Y. Tokura, Metal-insulator transitions, Rev. Mod. Phys. **70**, 1039 (1998).

[15] J. Hubbard, Electron correlations in narrow energy bands, Proc. R. Soc. London, Ser. A **276**, 238 (1963).

[16] A. Geroges, G. Kotliar, W. Krauth, and M. J. Rozenberg, Dynamical mean-field theory of strongly correlated fermion systems and the limit of infinite dimensions, Rev. Mod. Phys. **68**, 13 (1996).

[17] G. D. Mahan, Good thermoelectrics, Solid State Phys. **51**, 81 (1998).

[18] R. R. Heikes and R. W. Ure, *Thermoelectricity: Science and Engineering*, (Interscience Publishers, New York-London, 1961).

[19] P. M. Chaikin and G. Beni, Thermopower in the correlated hopping regime, Phys. Rev. B **13**, 647 (1976).

[20] J.-P. Doumerc, Thermoelectric power for carriers in localized states: A generalization of heikes and chaikin-beni formulae, J. Solid State Chem. **110**, 419 (1994).

[21] D. B. Marsh and P. E. Parris, Theory of the seebeck coefficient in $LaCrO_3$ and related perovskite systems, Phys. Rev. B **54**, 7720 (1996).

[22] D. B. Marsh and P. E. Parris, High-temperature thermopower of $LaMnO_3$ and related systems, Phys. Rev. B **54**, 16602 (1996).

[23] W. Koshibae, K. Tsutsui, and S. Maekawa, Thermopower in cobalt oxides, Phys. Rev. B **62**, 6869 (2000).

[24] B. N. Figgis and M. A. Hitchman, *Ligand Field Theory and Its Applications* (Wiley-VCH, Weinheim, 2000).

[25] Y. Tanabe and S. Sugano, On the absorption spectra of complex ions I, J. Phys. Soc. Jpn. **9**, 753 (1954).

[26] Y. Tanabe and S. Sugano, On the absorption spectra of complex ions II, J. Phys. Soc. Jpn. **9**, 766 (1954).

[27] J. S. Griffith, *The Theory of Transition-Metal Ions* (Cambridge University Press, London, 1971).

[28] J. C. Slater and G. F. Koster, Simplified LCAO method for the periodic potential problem, Phys. Rev. **94**, 1498 (1954).

[29] D. J. Singh, Electronic structure of $NaCo_2O_4$, Phys. Rev. B **61**, 13397 (2000).

[30] R. Kubo, Statistical-mechanical theory of irreversible processes. I. general theory and simple applications to magnetic and conduction problems, J. Phys. Soc. Jpn. **12**, 570 (1957).

[31] J. M. Luttinger, Theory of thermal transport coefficients, Phys. Rev. **135**, A1505 (1964).

[32] H. Matsuura, H. Maebashi, M. Ogata, and H. Fukuyama, Effect of phonon drag on seebeck coefficient based on linear response theory: Application to $FeSb_2$, J. Phys. Soc. Jpn. **88**, 074601 (2019).

[33] W. Koshibae and S. Maekawa, Effects of Spin and Orbital Degeneracy on the Thermopower of Strongly Correlated Systems, Phys. Rev. Lett. **87**, 236603 (2001).

[34] M. M. Zemljič and P. Prelovšek, Thermoelectric power in one-dimensional Hubbard model, Phys. Rev. B **71**, 085110 (2005).

[35] T. Okuda, K. Nakanishi, S. Miyasaka, and Y. Tokura, Large thermoelectric response of metallic perovskites: $La_{1-x}Sr_xTiO_3$ $(0 \leqslant x \leqslant 0.1)$, Phys. Rev. B **63**, 113104 (2001).

[36] A. V. Kovalevsky, A. A. Yaremchenko, S. Populoh, A. Weidenkaff, and J. R. Frade, Enhancement of thermoelectric performance in strontium titanate by praseodymium substitution, J. Appl. Phys. **113**, 053704 (2013).

[37] M. Uchida, K. Oishi, M. Matsuo, W. Koshibae, Y. Onose, M. Mori, J. Fujioka, S. Miyasaka, S. Maekawa, and Y. Tokura, Thermoelectric response in the incoherent transport region near Mott transition: The case study of $La_{1-x}Sr_xVO_3$, Phys. Rev. B **83**, 165127 (2011).

[38] D. P. Karim, and A. T. Aldred, Localized level hopping transport in $La(Sr)CrO_3$, Phys. Rev. B **20**, 2255 (1979).

[39] S. Pal, S. Hébert, C. Yaicle, C. Martin, and A. Maignan, Transport and magnetic properties of $Pr_{1-x}Ca_xCrO_3$ $(x = 0.0 - 0.5)$: Effect of t_{2g} orbital degeneracy on the thermoelectric power, Eur. Phys. J. B **53**, 5 (2006).

[40] T. T. M. Palstra, A. P. Ramirez, S-W. Cheong, B. R. Zegarski, P. Schiffer, and J. Zaanen, Transport mechanisms in doped $LaMnO_3$: Evidence for polaron formation, Phys. Rev. B **56**, 5104 (1997).

[41] W. Kobayashi, I. Terasaki, M. Mikami, and R. Funahashi, Negative thermoelectric power induced by positive carriers in $CaMn_{3-x}Cu_xMn_4O_{12}$, J. Phys. Soc. Jpn. **73**, 523 (2004).

[42] J. Mizusaki, T. Sasamoto, W. R. Cannon, and H. K. Bowen, Electric conductivity, Seebeck coefficient, and defect structure of $La_{1-x}Sr_xFeO_3$ $(x = 0.1, 0.25)$, J. Am. Ceram. Soc. **66**, 247 (1983).

[43] K. Berggold, M. Kriener, C. Zobel, A. Reichl, M. Reuther, R. Müller, A. Freimuth, and T. Lorenz, Thermal conductivity, thermopower, and figure of merit of $La_{1-x}Sr_xCoO_3$, Phys. Rev. B **72**, 155116 (2005).

[44] Y. Wang, Yu Sui, P. Ren, L. Wang, X. Wang, W. Su, and H. J. Fan, Correlation between the structural distortions and thermoelectric characteristics in $La_{1-x}A_xCoO_3$ (A = Ca and Sr), Inorg. Chem. **49**, 3216 (2010).